LETTER

Experimental and theoretical explorations for optimizing high-power geometric modes in diode-pumped solid-state lasers

IOP Publishing | Astro Ltd
Laser Physics Letters
Laser Phys. Lett. **15** (2018) 075802 (6pp)
https://doi.org/10.1088/1612-202X/aac29c

Letter

Experimental and theoretical explorations for optimizing high-power geometric modes in diode-pumped solid-state lasers

Y H Hsieh[1], Y H Lai[1], C H Tsou[1], H C Liang[2], K F Huang[1] and Y F Chen[1,3]

[1] Department of Electrophysics, National Chiao Tung University, Hsinchu 30010, Taiwan
[2] Institute of Optoelectronic Science, National Taiwan Ocean University, Keelung 20224, Taiwan
[3] Department of Electrophysics, National Chiao Tung University, 1001 TA Hsueh Road, Hsinchu 30010, Taiwan

E-mail: yfchen@cc.nctu.edu.tw

Received 20 April 2018, revised 30 April 2018
Accepted for publication 3 May 2018
Published 1 June 2018

Abstract

The variation of transverse patterns on the cavity length is experimentally explored by using an off-axis pumped Nd:YVO_4 laser to identify the range of the length for generating geometric modes (GMs). Using the inhomogeneous Helmholtz equation, it is theoretically confirmed that the stable range of the cavity length for generating GMs can be significantly enlarged by decreasing the output reflectance. Furthermore, experimental results reveal that the cavity length for scaling up the output power of GMs must be shortened due to the thermal lensing effect in the gain medium. Considering the balance between the output efficiency and the stable range of the cavity length, the optimal output reflectance is verified to be approximately 80%. With the optimal output reflectance, the average output power of GMs can be up to 6.33 W at a pump power of 12 W.

Keywords: geometric mode, diode-pumped, solid-state laser

(Some figures may appear in colour only in the online journal)

1. Introduction

Since Herriott *et al* [1] discovered that the off-axis incident beam could form a closed ray orbit in a two-mirror resonator, these so-called geometric mode (GMs) which represented the ray dynamics of light were widely exploited in several applications such as optical delay lines [2], achieving ultrafast lasers [3–5], and on-chip infrared spectroscopic sensors [6]. In the past two decades, it has been found that the solid-state lasers with off-axis pumping scheme can generate high-order transverse modes [7] which form GMs when the cavity length are close to the degenerate cavities [8–11]. The degenerate condition requires the ratio of transverse mode spacing to longitudinal mode spacing being a rational number P/Q. The generated GMs can be further converted to circular GMs with large orbital angular momentum and a particular optical vortex structure by using an astigmatic cylindrical lens [12–14] as shown in figure 1(a) for $(P,Q) = (1,4)$. Figures 1(b)–(c) illustrate the calculated wave pattern and the vortex structure of the circular GM based on the theory in the [14]. The structured beams have potential in applications such as the microparticle manipulation [15], the fabrication of twisted metal nanostructure [16, 17], and the quantum communication [18, 19]. For practical applications, the scalability of output power of GMs is a crucial issue. Under the high-power operation of the ended pumped solid-state laser, the unused pump power usually gives rise to the thermal lens effect due to the thermal expansion and thermally induced refractive index change in gain medium [20]. The thermal lens effect will cause decrease in efficiency, in beam quality, and shortened degenerate cavity

length [21, 22]. The last will render the initial degenerate cavity condition obsolete, which leads to deteriorated morphologies for GMs. Therefore, thermal lens effect must be put into consideration and optical cavity needs to be optimized accordingly to generate stable, high-power GMs with transverse wave patterns reliably.

Recently, the theoretical model based on the inhomogeneous Helmholtz equation is developed to reconstruct all experimental transverse patterns of GMs in the fractional degenerate cavities [8]. The agreement between theoretical calculations and experimental results provides the feasibility to analyze the transverse patterns of GMs near the degenerate cavities. Thus, the range of cavity length with stable structure of GMs can be systematically investigated and further exploited to optimize the cavity design for achieving high-power stable GMs. In this work, we experimentally explore the transverse patterns with the variation of the cavity length near the degenerate cavity by using an off-axis pumped Nd:YVO_4 laser to identify the range of the cavity length for the generation of GMs. We further utilize the inhomogeneous Helmholtz equation with the localized pump distribution to derive the GMs as a superposition of nearly degenerate and degenerate eigenmodes to reconstruct the experimental transverse patterns. With the experimental and theoretical results, the degree of the similarity between wave patterns is calculated to quantitatively characterize the stable range of the cavity length for generating GMs. It is found that the stable range can be significantly enlarged by decreasing the reflectance of the output coupler. For scaling up the output power, the experimental and theoretical results indicate that the cavity length of GMs must be shortened because of the thermal lensing effect in the gain medium. The optimal values of output reflectance is verified to 80% for a trade-off between the output efficiency and the stable range of the cavity length. With the optimal output reflectance, the average output power of GMs is up to 6.33 W at a pump power of 12 W.

2. Exploring the range of the cavity length for generating of the GMs

The experimental setup for observing transverse patterns to explore the range of cavity length for the generation of GMs is shown in figure 2. The laser medium was an *a*-cut 0.25-at.% Nd:YVO_4 crystal with length of 9 mm. Both sides of the Nd:YVO_4 crystal were coated for antireflection at 1064 nm (reflection <0.1%). The laser crystal was wrapped with indium foil and mounted in water-cooled copper holders with temperature stabilized at 16 °C. The gain medium was placed near the concave mirror with a separation about 2–3 mm. The input concave mirror had a high-reflectance coating at 1064 nm (reflection >99.8%) with the radius of curvature being $R = 30$ mm. The output coupler was a flat mirror with a reflectance $R_{oc} = 80\%$ at 1064 nm. In the concave-plano cavity, the ratio between transverse mode spacing Δf_T to longitudinal mode spacing Δf_L is given by $\Delta f_T/\Delta f_L = [(1/\pi)\sin^{-1}(\sqrt{L/R})]$ [8]. The condition for the degenerate cavity is written as $\Delta f_T/\Delta f_L = P/Q$, where P and Q are co-prime integers. In the present study, the cavity length of the degenerate cavity for $(P,Q) = (1,4)$ was given by $L_{1/4} = R[\sin(\pi/4)]^2 = 0.5R$. The pump source was an 808 nm fiber-coupled laser diode with a core diameter of 100 μm, a numerical aperture of 0.16, and a maximum output power of 20 W. A focus lens with a 38 mm focal length and 94% coupling efficiency was used to reimage the pump beam into the laser crystal. The pump radius was estimated to be 130 μm. The pumping beam was initially aligned at the transverse center of the laser cavity to excite the fundamental Gaussian mode. Subsequently, the pumping beam was displaced in the x direction by Δx to generate high-order modes. The lasing modes naturally became GMs with the sufficiently large off-axis displacement Δx [9].

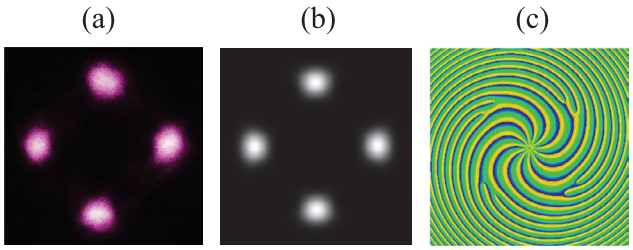

Figure 1. (a) The experimental transformed circular GM for $(P,Q) = (1,4)$ by using an astigmatic cylindrical converter. (b) and (c) the calculated wave pattern and the vortex structure of the circular GM based on the theory in the [14].

The transverse pattern of the GMs were observed in the far field region at $z = 40$ cm. The first row in the figure 3 is the variation of transverse patterns on the cavity length from −0.045 mm to 0.045 mm with respect to the degenerate cavity for $\Delta x = 0.5$ mm and the incident pump power $P_{in} = 2$ W. It can be seen that the localized spots corresponding to the GM, albeit spreading out as the displacement from the degenerate cavity $L_{1/4}$ becomes larger, are able to maintain their structural similarity. Therefore, the range of cavity length for the generation of GMs can be identified as 0.09 mm. To further analyze the experimental transverse patterns, the lasing resonant modes based on the inhomogeneous equation are discussed in the following paragraphs.

The laser cavity is supposed to be formed by a gain medium, a concave spherical mirror, and a plane output coupler. By using the paraxial approximation, the eigenmodes for the cavity with a concave mirror at $z = -L$ and a plane mirror at $z = 0$ are solved to be [23]

$$\psi_{n,m,l}^{(HG)}(x,y,z) = \sqrt{\frac{2}{L}}\Phi_{n,m}(x,y,z)\sin\left[k_{n,m,l}\tilde{z} - (n+m+1)\tan^{-1}(z/z_R)\right], \quad (1)$$

where

$$\Phi_{n,m}(x,y,z) = \frac{1}{\sqrt{2^{n+m-1}\pi n!m!}}\frac{1}{w(z)}H_n\left[\frac{\sqrt{2}x}{w(z)}\right]H_m\left[\frac{\sqrt{2}y}{w(z)}\right]. \quad (2)$$

Here $H(\cdot)$ is the Hermite polynomials of order n, $k_{n,m,l} = 2\pi f_{n,m,l}/c$, $f_{n,m,l}$ is the eigenmode frequency, $z_R = \sqrt{L(R-L)}$ is the Rayleigh range, R is the radius of cur-

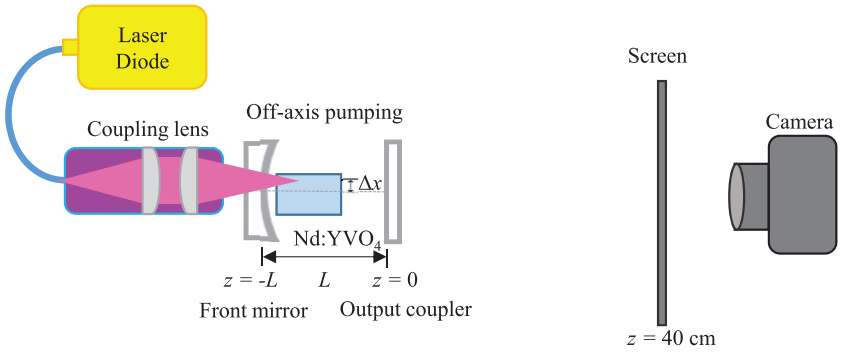

Figure 2. Configuration of the concave-plano cavity for employ the off-axis pumped Nd:YVO_4 laser in degenerate resonator. The CCD camera is used to record the far-field transverse patterns.

vature of the concave mirror, $\tilde{z} = z + [(x^2 + y^2)]/[2(z^2 + z_R^2)]$, $w(z) = w_o\sqrt{1 + (z/z_R)^2}$, and $w_o = \sqrt{\lambda z_R/\pi}$ is the beam radius at the waist. The eigenmode frequency of the spherical cavity is given by $f_{n,m,l} = [l\Delta f_L + (n + m + 1)\Delta f_T]$, where l is the longitudinal mode number, and n and m are the transverse mode numbers. For the mode-spacing ratio $\Omega = \Delta f_T/\Delta f_L$ being a rational number P/Q, it can be found that $f_{n,m,l}/\Delta f_L = M/Q$ with $M = [lQ + (n + m + 1)P]$ which can be satisfied by many combinations of (n,m,l) for a given number of M. The combinations of (n,m,l) constitute a degenerate group which proved to be intimately related to the emergence of the localized wave pattern [24–26]. Considering a locally pumped laser system, the lasing modes can be derived from the inhomogeneous Helmholtz equation:

$$(\nabla^2 + \tilde{k}^2)\Psi(x, y, z) = \eta_c F(x, y, z), \tag{3}$$

where $\tilde{k} = k + i\alpha$, $k = 2\pi/\lambda$ is the wave number of the emission light, and η_c represents the conversion efficiency for the pump source. α is a small loss parameter including loss from the scattering, the absorption, and the output coupling. Since the lasing modes are subject to the same boundary condition as the homogeneous Helmholtz equation for Hermite–Gaussian (HG) modes, the lasing modes and the source distribution can be written as the expansion of HG modes:

$$\Psi(x, y, z) = \sum_{n,m,l} a_{n,m,l}\psi^{(HG)}_{n,m,l}(x, y, z) \tag{4}$$

and

$$\eta_c F(x, y, z) = \sum_{n,m,l} b_{n,m,l}\psi^{(HG)}_{n,m,l}(x, y, z). \tag{5}$$

Substituting equations (4) and (5) into (3), the coefficient $a_{n,m,l}$ can be deduced to be: $a_{n,m,l} = b_{n,m,l}/(\tilde{k}^2 - k^2_{n,m,l})$. With the orthonormal property of eigenmodes, the coefficient $b_{n,m,l}$ is given by

$$b_{n,m,l} = \eta_c \iiint \psi^{(HG)}_{n,m,l}(x, y, z)F(x, y, z)dxdydz. \tag{6}$$

The pump source distribution $F(x,y,z)$ is considered to be approximately uniform in the longitudinal z axis. Thus, the coefficient $b_{n,m,l}$ related to the source distribution can be regarded as independent of index l in the neighborhood of the central index l_o and the radius of the pump beam can be

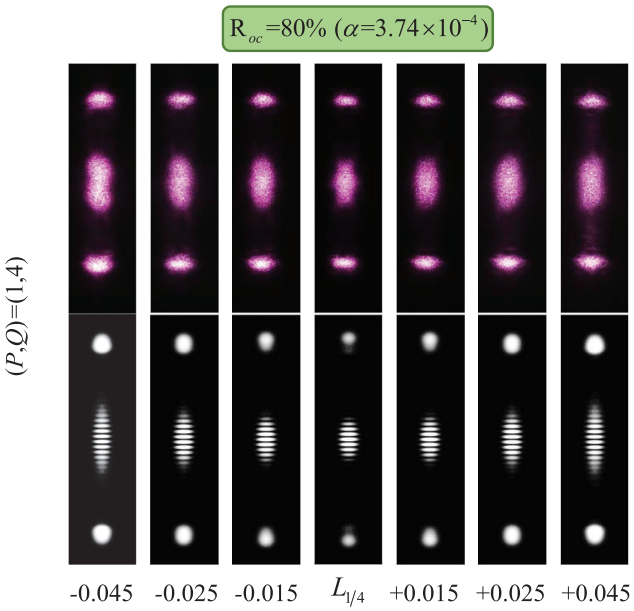

Figure 3. The first row is the variation of transverse patterns on the cavity length from −0.045 mm to 0.045 mm with respect to the degenerate cavity $L_{1/4}$ for $\Delta x = 0.5$ mm and the incident pump power $P_{in} = 2$ W. The second row is calculated transverse patterns of $|\Psi(x, y, z)|^2$ with given parameters $R = 30$ mm, $\lambda = 1064$ nm, $\alpha = 3.74 \times 10^{-4}$ ($R_{oc} = 80\%$, $\Gamma = 1 \times 10^{-3}$), and $n_o = 50$.

viewed as a constant $w(z_c)$ in the range $|z - z_c| \leqslant L_c/2$, where z_c is the location of the gain medium and L_c is the length of the gain medium. On the other hand, the transverse distribution of the source is assumed to be the Gaussian distribution. As a result, the $F(x,y,z)$ for the off-axis pumping of the transverse displacement Δx can be expressed as

$$F(x, y, z) = \frac{1}{L_c}\frac{2}{\pi w^2(z_c)}\exp\left[-\frac{(x - \Delta x)^2 + y^2}{w^2(z_c)}\right]. \tag{7}$$

Substituting the equations (1), (2) and (7) into the (6) and using the generating function of the Hermite polynomials, the coefficient $b_{n,m,l}$ can be derived to be $b_{n,m,l} = (\eta/L_c)[\sqrt{2/\pi w^2(z_c)}][(n_o)^{n/2} e^{-n_o/2}/\sqrt{n!}]\delta_{m,0}$, where η is a constant that includes the effective conversion η_c and the overlap integral in the longitudinal direction, and $n_o = [\Delta x/w(z_c)]^2$. The expression $(n_o)^{n/2} e^{-n_o/2}/\sqrt{n!}$ is the form of the square root of the Poisson distribution which indicates that the

maximum contribution in the resonant states is the eigenmode with order n to be the most immediate integer to the value n_o. Note that it also has been found that the high-order HG mode can be generated in the off-axis pumped solid-state lasers with $n = [\Delta x/w(z_c)\,]^2$. The Poisson distribution can be approximately expressed as the Gaussian distribution for large value of n_o from the central limit theorem. Thus, the $b_{n,m,l}$ can be derived as

$$b_{n,m,l} = \frac{\eta}{L_c}\sqrt{\frac{2}{\pi w^2(z_c)}}\frac{1}{\sqrt{\sqrt{2\pi n_o}}}\exp\left[-\frac{(n-n_o)^2}{4n_o}\right]\delta_{m,0}. \tag{8}$$

With the property of Gaussian distribution, the effective range of the mode order n is limited to $|n - n_o| \leqslant N$ with $N = 2\sqrt{n_o}$. Substituting the expression of $b_{n,m,l}$ in equation (8) into $a_{n,m,l} = b_{n,m,l}/(\tilde{k}^2 - k^2_{n,m,l})$ with $\alpha \ll k$ and $k = \pi[l_o + (n_o + 1)]/L$, the resonant lasing modes in the equation (4) can be further deduced to be

$$\begin{aligned}\Psi(x,y,z) &= \sum_{n,m,l}\frac{b_{n,m,l}}{(k^2-k^2_{n,m,l})+2i\alpha k}\psi^{(HG)}_{n,m,l}(x,y,z)\\ &= \frac{\eta\lambda L}{4\pi^2 L_c}\sqrt{\frac{2}{\pi w^2(z_c)}}\frac{1}{\sqrt{\sqrt{2\pi n_o}}}\\ &\left\{\sum_{l=l_o-J}^{l_o+J}\sum_{n=n_o-N}^{n_o+N}\frac{\exp[-(n-n_o)^2/4n_o\,]}{[(l_o-l)+(n_o-n)\Omega]+i\gamma}\psi^{(HG)}_{n,m,l}(x,y,z)\right\},\end{aligned} \tag{9}$$

where J is associated with the effective range of the longitudinal order l and $\gamma = \alpha L/\pi$. The equation (9) indicates that the degenerate or nearly degenerate modes dominate the superposition for the formation of resonant modes. The nearly degenerate condition requires the index J being an integer closest to $N\Omega$. Additionally, the loss parameter α can be generalized as $\alpha = (n_o/l_o)\,[\ln(1/R_{oc}\,) + \Gamma]$, where Γ is a small constant related to nonsaturable intracavity round-trip dissipative optical loss. The second row in figure 3 demonstrates the calculated transverse patterns of $|\Psi(x,y,z)|^2$ with given parameters $R = 30\,\text{mm}$, $\lambda = 1064\,\text{nm}$, $\alpha = 3.74\times10^{-4}$ ($R_{oc} = 80\%$, $\Gamma = 1\times10^{-3}$), and $n_o = 50$. The good agreement between the experimental and theoretical results provides convincing proof for the experimental identification of the stable range of the cavity length.

In order to quantitatively characterize the stable range of the cavity length, the spatial correlation coefficient related to the degree of the similarity between the wave patterns near the degenerate cavity is further calculated by using $C = \int f(\vec{r})g(\vec{r})d\,\vec{r}$ [27], where $f(\vec{r})$ and $g(\vec{r})$ are normalized with respect to the spatial coordinates. The two functions are highly similar when the value of C approaches 1. Here we set $g(\vec{r})$ to be the resonant mode at $L_{1/4}$ whereas $f(\vec{r})$ to be the mode at $L_{1/4} + \Delta L$. Figure 4 demonstrates the degree of the similarity versus the variation of the cavity length. The red line is the calculated result for $\alpha = 3.74\times10^{-4}$ ($R_{oc} = 80\%$) that shows the gradual decrease for $\Delta L \leqslant 0.013$ mm and $\Delta L \geqslant 0.028$ mm, and the steep drop for $0.013\,\text{mm} \leqslant \Delta L \leqslant 0.028\,\text{mm}$. We require the value of C being higher than 0.8 according to the identified range of the cavity length for generating GMs in figure 3. Therefore,

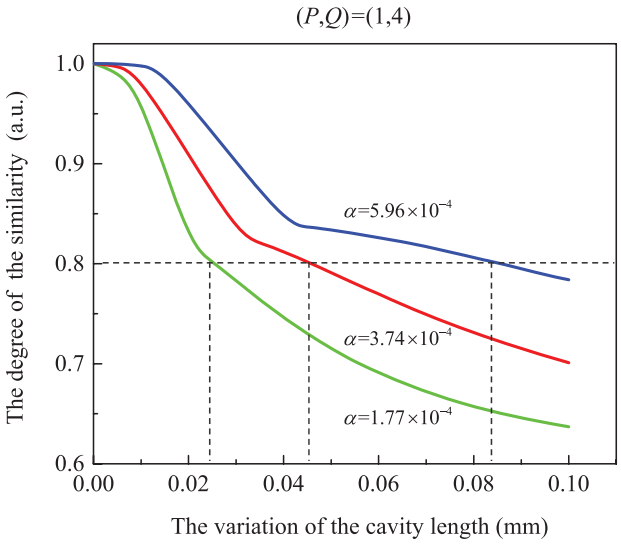

Figure 4. The calculated degree of the similarity versus the variation of the cavity length for $\alpha = 3.74\times10^{-4}$ ($R_{oc} = 80\%$), $\alpha = 1.77\times10^{-4}$ ($R_{oc} = 90\%$) and $\alpha = 5.96\times10^{-4}$ ($R_{oc} = 70\%$).

the stable range of the cavity length can be determined. Considering different output reflectance, the experimental transverse patterns with the variation of cavity length are verified by theoretical calculations with different loss parameter for $\alpha = 1.77\times10^{-4}$ ($R_{oc} = 90\%$) and $\alpha = 5.96\times10^{-4}$ ($R_{oc} = 70\%$), respectively. Then, the corresponding degree of similarity are calculated and shown in figure 3. The lower the output reflectance is, the wider the range of cavity length for generating GMs is. In other words, the wide range of cavity length is resulted from the laser cavity approaching an open system. In other optical systems such as the microcavity lasers, the openness of the system has significant influence on generating lasing modes with the strong directional emission and the concentrated transverse patterns along ray trajectories [28–31]. In the following section, we analyze the shift of the degenerate cavity as the power increases to find the criterion for generating high-power GMs.

3. The optimization of the GMs

For scaling up the output power of GMs, the shift of the degenerate cavity resulted from the thermal lensing effect is first analyzed. We measure the stable range at $R_{oc} = 80\%$ for $(P,Q) = (1,4)$ with its center recorded as the degenerate cavity. Then, the degenerate cavity with pump power $P_{in} = 1\,\text{W}$ is set to be the reference to determine the shift of the degenerate cavity $\Delta L_{1/4}$ due to the weak thermal lens effect under the low power operation. Figure 5 displays the shift of the degenerate cavity $\Delta L_{1/4}$ versus the incident pump power. The histogram represents the range of the cavity length for the generation of GMs and the red circle in the center of the histogram is the degenerate cavity. It can be seen that the length of the degenerate cavity is shortened by 0.09 mm with $P_{in} = 12$ W. Since the stable range of cavity length is larger than the shift of degenerate cavity, we can observe from the blue dashed line that the degenerate cavity at $P_{in} = 8$ W maintain a stable

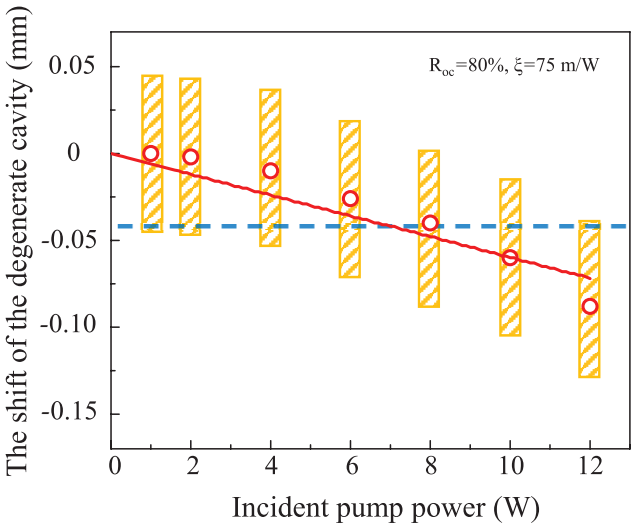

Figure 5. The experimental stable range and shift of the degenerate cavity $\Delta L_{1/4}$ versus the incident pump power with the fitted curve solved from equation (10).

structure of GM for $P_{in} \leqslant 12$ W. We then theoretically analyze the shift of the degenerate cavity by using ray transfer matrix of the optical cavity containing a lens with the focal length f:

$$M(L) = \begin{bmatrix} A & B \\ C & D \end{bmatrix} = \begin{bmatrix} 1 - \frac{2L}{f} & 2L \\ \left(\frac{2}{R} + \frac{1}{f}\right)\left(\frac{2L}{f} - 1\right) & \left(\frac{2}{R} + \frac{1}{f}\right)(1 - 2L) \end{bmatrix}. \tag{10}$$

Note that the focal length can be expressed as a function of the pump power to be: $f = \xi / P_{in}$ [19], where ξ is a constant sensitivity factor. For a stable cavity, the trace of the round-trip transfer matrix for the resonator should satisfy the criterion $|\cos\theta = (A + D)/2| \leqslant 1$ with the position $x_s = x_o \sin(s\theta + \phi_o)$, where x_o is the maximum displacement with respect to the x-axis, and ϕ_o is related to the initial position. The Q-fold periodic ray orbit requires the paraxial ray return to its original position after Q round-trips: $Q\theta = 2N\pi$, where $N = 0, \pm 1, \pm 2, \ldots$. As a result, the phase angle θ can be expressed as $\theta = 2\pi P/Q$ without loss of generality. For $(P,Q) = (1,4)$, the theoretical degenerate cavity length in terms of pump power $L_{1/4}(P_{in})$ can be solved by $\cos(\pi/2) = (A + D)/2$ with a given ξ factor. Subsequently, the shift of the cavity length is decided by $\Delta L_{1/4}(P_{in}) = L_{1/4}(P_{in}) - L_{1/4}(P_{in} \to 0)$. The calculated shift of the degenerate cavity, depicted as a red line in the figure 5, is fitted to best describe the experimental data. It is worthy to note that the degree of factor ξ under the off-axis pumping is much longer than that of on-axis pumping scheme, being at tens of meter per watt and tens of centimeter per watt [20], respectively. The focal length can be considered to be independent of the output reflectance. Therefore, the output reflectance is found should be smaller than or equal to 80% for obtaining the stable range of cavity length larger than the shift of degenerate cavity.

Next, several flat output couplers with different output reflectance in the range of $30\% \leqslant R_{oc} \leqslant 98\%$ are used to explore the influence of the output coupler on the lasing performance.

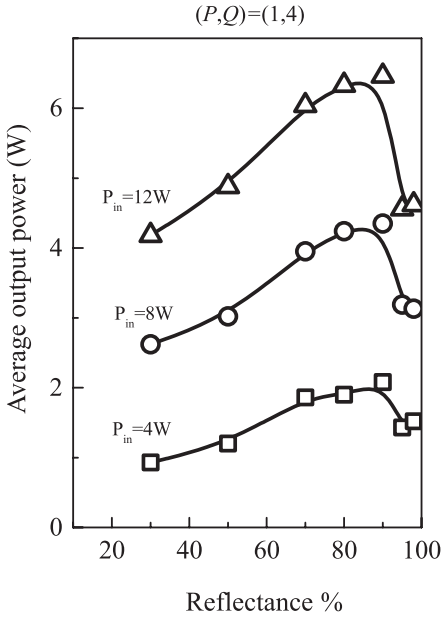

Figure 6. The experimental dependences of the average output power on the output reflectance for several incident pump powers for $(P,Q) = (1,4)$.

Figure 6 displays the dependence of the average output power on the reflectance of the output coupler for several incident pump power. Here the cavity length is set to be $L_{1/4}$ for each pump power. Note that the average output power is nearly the same for the cavity length being adjusted to the degenerate cavity at various pump power and being a fixed value subject to the degenerate cavity at a certain pump power. It can be seen that the optimum R_{oc} is approximately 90% for the pump power of less than 12 W. However, the optimum value of R_{oc} is modified to be at 80% for making a balance between the stable range of cavity length and the output efficiency. Consequently, the maximum output power of stable GMs can be up to 6.33 W at $R_{oc} = 80\%$ under the incident pump power of 12 W. The accomplishment of high-power stable GMs is believed to enhance the feasibility in various practical applications.

4. Conclusions

In conclusion, we have experimentally explored the variation of transverse patterns on the cavity length near the degenerate cavity by exploiting an off-axis pumped Nd:YVO_4 laser to identify the range of the length for generating GMs. We have been utilized the inhomogeneous Helmholtz equation with the localized source distribution to reconstruct the experimental wave patterns. It is experimentally and theoretically confirmed that the stable range of cavity length significantly increases by decreasing the output reflectance. For scaling the output power of GMs, the degenerate cavity is observed to be shortened due to the thermal lensing effect in the gain medium. The optimal value of output reflectance is found to be approximate 80% for making a compromise between the output efficiency and the stable range of cavity length. With the optimal reflectance, the average output power of stable GMs is up to 6.33 W

at a pump power of 12 W. As far as we know, this is the highest efficiency for generating high-power GMs. The achievement of high-power stable GMs is believed to be practically valuable in further applications.

Acknowledgments

This work is supported by the Ministry of Science and Technology of Taiwan (Contract No. MOST105-2628-M-009-004).

References

[1] Herriott D R, Kogelnik H and Kompfner R 1964 Off-axis paths in spherical mirror interferometers *Appl. Opt.* **3** 523–6
[2] Herriott D R and Schulte H J 1965 Folded optical delay lines *Appl. Opt.* **4** 883–9
[3] Sennaroglu A, Kowalevicz A M, Ippen E P and Fujimoto J G 2004 Compact femtosecond lasers based on novel multi-pass cavities *IEEE J. Quantum Electron.* **40** 519–28
[4] Godil A A, Auld B A and Bloom D M 1994 Picosecond time-lenses *IEEE J. Quantum Electron.* **30** 827–37
[5] Saraceno C J, Emaury F, Schriber C, Diebold A, Hoffmann M, Golling M, Südmeyer T and Keller U 2015 Toward millijoule-level high-power ultrafast thin-disk oscillators *IEEE J. Sel. Top. Quantum Electron.* **21** 106–23
[6] Kita D, Lin H, Agarwal A, Richardson K, Luzinov I, Gu T and Hu J 2017 On-chip infrared spectroscopic sensing: redefining the benefits of scaling *IEEE J. Sel. Top. Quantum Electron.* **23** 5900110
[7] Chen Y F, Huang T M, Kao C F, Wang C L and Wang S C 1997 Generation of Hermite-Gaussian modes in fiber-coupled laser-diode end-pumped lasers *IEEE J. Quantum Electron.* **33** 1025–31
[8] Chen Y F, Tung J C, Chiang P Y, Liang H C and Huang K F 2013 Exploring the effect of fractional degeneracy and the emergence of ray-wave duality in solid-state lasers with off-axis pumping *Phys. Rev.* A **88** 013827
[9] Chen Y F, Chang C C, Lee C Y, Sung C L, Tung J C, Su K W, Liang H C, Chen W D and Zhang G 2017 High-peak-power large-angular-momentum beams generated from passively Q-switched geometric modes with astigmatic transformation *Photon. Res.* **5** 561–6
[10] Chen Y F, Jiang C H, Lan Y P and Huang K F 2004 Wave representation of geometrical laser beam trajectories in a hemiconfocal cavity *Phys. Rev.* A **69** 053807
[11] Tung J C, Liang H C, Tuan P H, Chang F L, Huang K F, Lu T H and Chen Y F 2016 Selective pumping and spatial hole burning for generation of photon wavepackets with ray-wave duality in solid-state lasers *Laser Phys. Lett.* **13** 025001
[12] Sridhar H, Cohen M G and Noé J W 2010 Creating optical vortex modes with a single cylinder lens *Proc. SPIE* **7613** 33
[13] Nam H A, Cohen M G and Noé J W 2011 A simple method for creating a robust optical vortex beam with a single cylinder lens *J. Opt.* **13** 064026
[14] Tung J C, Liang H C, Lu T H, Huang K F and Chen Y F 2016 Exploring vortex structures in orbital-angular-momentum beams generated from planar geometric modes with a mode converter *Opt. Express* **24** 22796–805
[15] Gahagan K T and Swartzlander G A Jr 1996 Optical vortex trapping of particles *Opt. Lett.* **21** 827–9
[16] Toyoda K, Miyamoto K, Aoki N, Morita R and Omatsu T 2012 Usingoptical vortex to control the chirality of twisted metal nanostructures *Nano Lett.* **12** 3645–9
[17] Toyoda K, Takahashi F, Takizawa S, Tokizane Y, Miyamoto K, Morita R and Omatsu T 2013 Transfer of light helicity to nanostructures *Phys. Rev. Lett.* **110** 143603
[18] Molina-Terriza G, Torres J P and Torner L 2007 Twisted photons *Nat. Phys.* **3** 305–10
[19] Gibson G, Courtial J, Padgett M J, Vasnetsov M, Pas'ko V, Barnett S M and Franke-Arnold S 2004 Free-space information transfer using light beams carrying orbital angular momentum *Opt. Express* **12** 5448–56
[20] Koechner W 1971 *Solid State Laser Engineering* (Berlin: Springer) p 442
[21] Song F, Zhang C, Ding X, Xu J and Zhang G 2002 Determination of thermal focal length and pumping radius in gain medium in laser-diode-pumped Nd:YVO_4 lasers *Appl. Phys. Lett.* **81** 2145–7
[22] Ozygus B and Zhang Q 1997 Thermal lens determination of end-pumped solid-state lasers using primary degeneration modes *Appl. Phys. Lett.* **71** 2590–2
[23] Siegman A E 1986 *Lasers* (Mill Valley, CA: University Science)
[24] Hsieh Y H, Yu Y T, Tuan P H, Tung J C, Huang K F and Chen Y F 2017 Extracting trajectory equations of classical periodic orbits from the quantum eigenmodes in two-dimensional integrable billiards *Phys. Rev.* E **95** 053807
[25] Roy S M and Singh V 1982 *Phys. Rev.* D **25** 3413
[26] Zhang W M and Gilmore R 1990 *Rev. Mod. Phys.* **62** 867–927
[27] Goshtasby A A 2012 *Image Registration: Principles, Tools and Methods* (Berlin: Springer) p 7
[28] Lee S B, Lee J H, Chang J S, Moon H J, Kim S W and An K 2002 Observation of scarred modes in asymmetrically deformed microcylinder lasers *Phys. Rev. Lett.* **88** 033903
[29] Lee S Y, Rim S, Ryu J W, Kwon T Y, Choi M and Kim C M 2004 Quasiscarred resonances in a spiral-shaped microcavity *Phys. Rev. Lett.* **93** 164102
[30] Lee S-Y, Ryu J-W, Kwon T-Y, Rim S and Kim C-M 2005 Scarred resonances and steady probability distribution in a chaotic microcavity *Phys. Rev.* A **72** 061801
[31] Wiersig J and Hentschel M 2008 Combining directional light output and ultralow loss in deformed microdisks *Phys. Rev. Lett.* **100** 033901